CHEMBIOCHEM

Supporting Information

Discovery of New Classes of Compounds that Reactivate Acetylcholinesterase Inhibited by Organophosphates

Francine S. Katz,*[a] Stevan Pecic,[a] Timothy H. Tran,[b] Ilya Trakht,[a] Laura Schneider,[a] Zhengxiang Zhu,[a] Long Ton-That,[a] Michal Luzac,[a] Viktor Zlatanic,[a] Shivani Damera,[a] Joanne Macdonald,[a, c] Donald W. Landry,[a] Liang Tong,*[b] and Milan N. Stojanovic[a, d]

cbic_201500348_sm_miscellaneous_information.pdf

Table of Contents

Supporting Information

Supplementary Methods and Materials

Solid-phase High-Throughput Screening Assay. Different formats for immobilization of AChE on 96-well plates were tested to determine efficiency of binding AChE to a surface while maintaining the active form of the enzyme. The indicated amounts of AChE were added per well and allowed to incubate overnight, after which any residual AChE that was not bound to the plate was washed away before testing for AChE activity by Ellman's assay[1], adding ATCh and DTNB (2mM each) and monitoring the rate of increase in absorbance at 412nm using a Spectramax384 plate reader. After testing for AChE activity, the plates were washed thoroughly and then probed with an anti-AChE antibody to determine how much enzyme was on the plate, in order to correlate the amount of enzyme with amount of active enzyme present. Initial rate of the breakdown of acetylthiocholine was measured by standard Ellman's assay (left), after which plates were probed for AChE protein using ELISA detection (right). NUNC plates with Nunclon™ Delta surface showed the highest overall activity and the best correlation between amount of enzyme present and enzyme activity, so we chose to carry out the screen using these conditions.

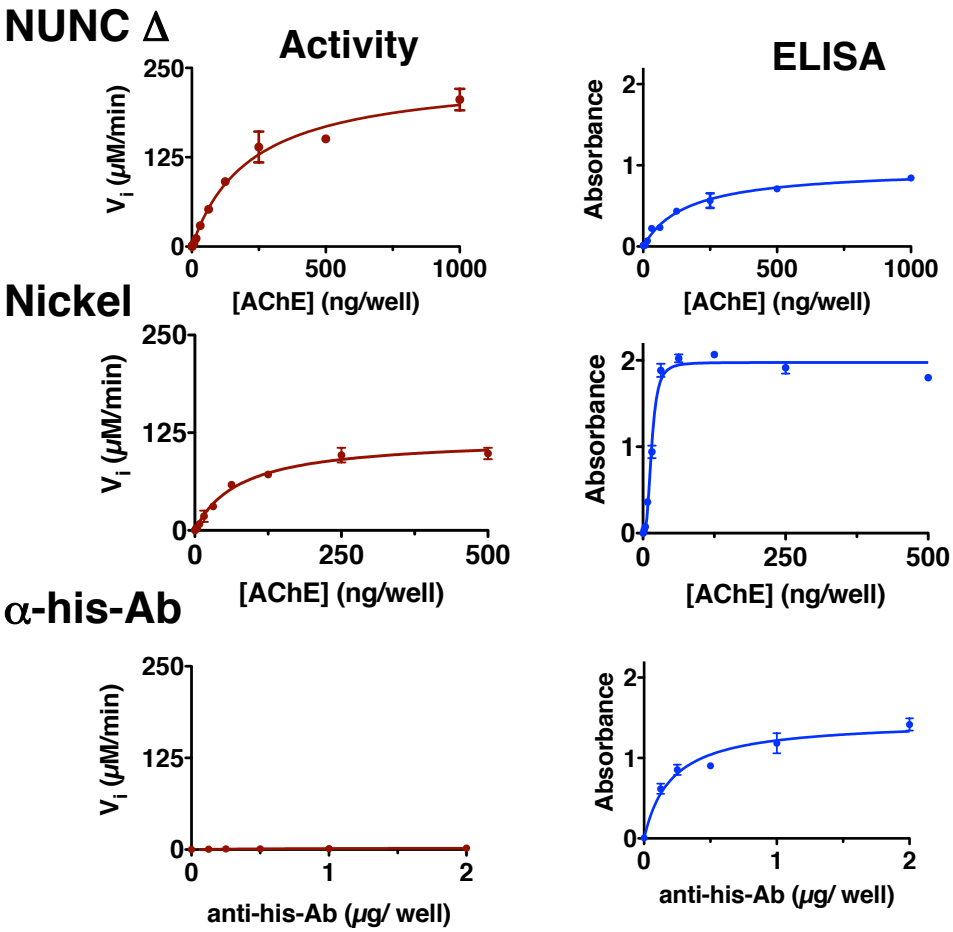

Figure S1. Test of screening platforms. Different formats for immobilization of AChE on 96-well plates were tested to determine efficiency to bind AChE and maintain activity. Initial rate of the breakdown of acetylthiocholine was measured by standard Ellman's assay (left), after which plates were probed for AChE protein using ELISA detection (right).

Determination of Reactivation Rate Constants. Reactivation rate constants were calculated based on a modification of previously published methods,[2] using the following scheme for reaction progression.

$$[E\bullet OPC] + [R] \overset{K_R}{\longleftrightarrow} [E\bullet OPC\bullet R] \xrightarrow{k_2} [E] + [OPC] + [R]$$

In this simplified scheme, [*E•OPC*] represents the OPC-bound form of AChE. Free enzyme, [E], can be restored by adding the reactivator, [R], that binds to the [*E•OPC*] complex with the apparent affinity constant (K_R). (The binding affinity to the free enzyme could possibly be different than K_R and is determined using standard assays that are used to determine the inhibition constant (K_i)). Increasing the concentration of R results in an increase in the rate of reactivation until it reaches saturation, or the maximum first order rate constant (k_2), with the overall reaction governed by the second order rate constant (k_r).

In a simple system, when R is present at much higher concentrations than the K_R, the first order rate constant for reactivation (k_{obs}) can be defined as:

$$k_{obs} = \frac{k_2\,[R]}{K_R + [R]}$$

And the second order rate constant (k_r), is derived using this equation:

$$k_r = \frac{k_2}{K_R}$$

It is important to note that the *E•OPC* complex can undergo other processes that would prevent reactivation or slow the apparent rate of reactivation over time, for example as in the dealkylative process of aging. In these cases, the reactivation reaction would follow the scheme below:

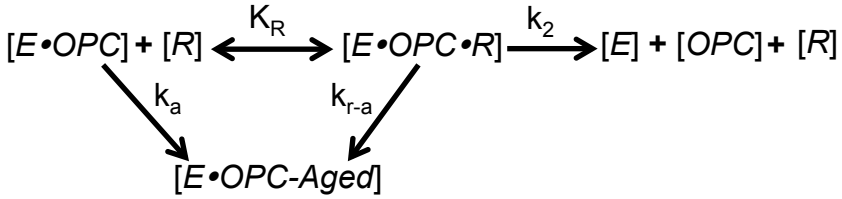

Here the [*E•OPC*] breaks down to [*E•OPC-Aged*] at the rate k_a which can be altered (either accelerated or decelerated) in the presence of reactivator, indicated as $k_{r\text{-}a}$. Because formation of [*E•OPC-Aged*] will reduce the amount of total enzyme that can be regenerated, it essentially reduces the amount of total enzyme, and k_{obs} is determined by fitting the data to a one phase association in which there is a maximum level of reactivation. That maximum is experimentally determined after measuring reactivation after extended incubation (% R_{max}). Experimentally determined % R_{max} values are listed in Table S1, we did not determine the rate of aging experimentally. These data can be fit to the standard equation:

$$(\%\ \text{Reactivation})_t = \%R_{max}\,(1 - e^{-k_{obs}\,t})$$

where k_{obs} is calculated from fitting experimental data measuring the % Reactivation at various times (t). Secondary plots of the concentration of the reactivator vs. k_{obs} were used to obtain second order rate constants, and values for k_2 and K_R.

We found in some cases, the saturation curves were better fit to a sigmoidal curve, consistent with requiring multiple molecules present in the active site to reach maximum reactivation. All reactions were done either in triplicate or in duplicate on multiple days (minimum of quadruplicate) and plotted with error bars to show standard deviation.

Chemistry (C)

Compounds **7a**, **9a**, **9b** and **9c** were synthesized as shown by the reaction schemes below.

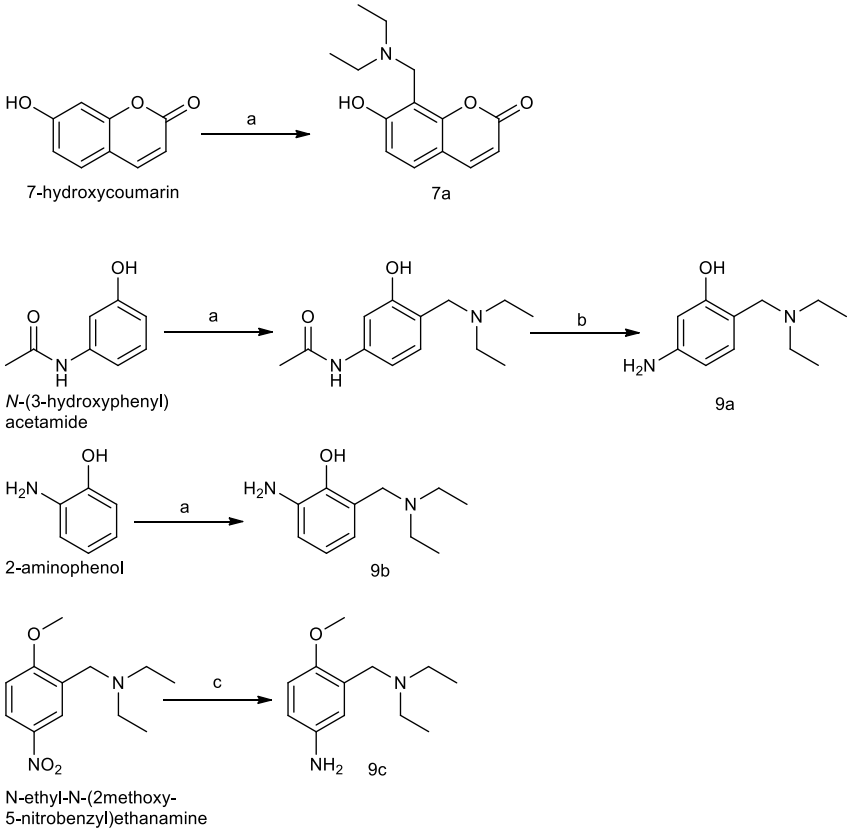

Scheme 1. *Reagents and conditions:* a) 37% aq. HCHO, Et_2NH, EtOH, reflux, 4-18 h; b) 3N HCl, reflux, 4h; c) PtO_2/H_2, EtOH, 4 h.

7-((diethylamino)methyl)-8-hydroxy-2H-chromen-2-one (7a). To a solution of the diethylamine (0.52 mL, 5 mmol) in 30 mL of absolute ethanol was added 37% aqueous formaldehyde solution (0.75 mL, 10 mmol). The solution was refluxed for 1 h and the 7-hydroxycoumarin was added (810 mg, 5 mmol), also dissolved in 30 mL of absolute ethanol. The reaction mixture was refluxed for 6 h, and stirred at RT overnight. The solvent was removed under reduced pressure. In order to remove starting material, crude product was treated with 1M HCl, and extracted with diethyl ether. Aqueous layer was basified with 1M NaOH, and title compound extracted with 2x25 mL ethyl acetate. Organic layers were combined, dried over Na_2SO_4, and concentrated to give **7a** as orange oil (650 mg, 55%). ^{1}H NMR (400 MHz, $CDCl_3$) δ 7.58 (d, *J*=9.2 Hz, 1H), 7.22 (d, *J*=8.4 Hz, 1H), 6.68 (d, *J*=8.4 Hz, 1H), 6.12 (d, *J*=9.6 Hz, 1H), 4.07 (s, 2H), 2.68 (q, J=7.2 Hz, 4H), 1.13 (t, *J*=7.2 Hz, 6H); ^{13}C NMR (100 MHz, $CDCl_3$) δ 164.2, 161.6, 153.2, 144.6, 127.9, 114.2, 111.0, 110.9, 108.1, 49.9, 46.9, 11.2; ESI-MS (*m/z+1)* 248.[7]

5-amino-2-((diethylamino)methyl)phenol (9a). 3-Hydroxyacetanilide (1 g, 6.615 mmol) was dissolved in ethanol (10 mL) in 100 mL round-bottom flask. Diethylamine (0.71 mL, 6.615 mmol) and 37% aqueous solution of formaldehyde (0.5 mL) was added to the reaction mixture and refluxed for 18 h. Solvent was removed under reduced pressure and the crude material was triturated in small amount of ethyl acetate. Light orange solid was filtered and used for next step without any further purification. It was dissolved in 3N HCl (5 mL) and solution heated under reflux for 4 h. The solvent was removed in vacuo (co-evaporated with ethyl acetate) to give **9a** as

hydrochloride salt. Free based compound **9a** was obtained by adding drop-wise solution of saturated $NaHCO_3$, until pH~8. Free base compound **9a** was then extracted with chloroform, organic layer was dried over Na_2SO_4, and concentrated to give pale desired compound **9a** as a yellow solid. (1.01 g, 77%, after two steps); mp 193-196 °C; ^{1}H NMR (400 MHz, $CDCl_3$) δ 6.72 (d, *J*=8.4 Hz, 1H), 6.17 (s, 1H), 6.11 (d, *J*=7.6 Hz, 1H), 4.68 (bs, 2H), 3.65 (s, 2H), 2.59 (q, *J*=6.8 Hz, 4H), 1.08 (t, *J*=7.2 Hz, 6H); ^{13}C NMR (100 MHz, $CDCl_3$) δ 159.2, 147.0, 129.0, 112.5, 105.9, 103.0, 56.5, 46.0, 11.2; ESI-MS (*m/z+1)* 195.[4]

2-amino-6-((diethylamino)methyl)phenol (9b). 2-Aminophenol (1.09 g, 10 mmol) was added to 100 mL round-bottom flask and dissolved in ethanol (30 mL), followed by diethylamine (1.04 mL, 10 mmol) and 37% aqueous formaldehyde solution (0.75 mL, 10 mmol) and the solution was allowed to heat under reflux for 4 h. After this reflux period, reaction mixture was cooled to O °C, and ice-cold water (20 mL) was added. Orange precipitate was filtered and dried overnight on house vacuum. Crude compound was dissolved in minimal amount of hot ethanol, and desired compound **9b** was recrystallized as dark red solid. (1.25 g, 64%); mp 192-194 °C; ^{1}H NMR (400 MHz, $CDCl_3$) δ 6.62-6.59 (m, 2H), 6.39 (d, *J*=9.2 Hz, 1H), 3.71 (s, 3H), 2.61 (q, *J*=7.2 Hz, 4H), 1.10 (t, *J*=7.2 Hz 6H); ^{13}C NMR (100 MHz, $CDCl_3$) δ 145.7, 134.9, 121.4, 118.8, 118.0, 114.3, 56.8, 46.2, 11.2; ESI-MS (*m/z+1)* 195.[5]

3-((diethylamino)methyl)-4-methoxyaniline (9c). Diethyl-(2-methoxy-5-nitro-benzyl)-amine, hydrochloride (50 mg, 0.18 mmol) was dissolved in ethanol (5 mL) and hydrogenated (1 atm) over platinum oxide (10 mg) for 4 hours. Reaction mixture was filtered through Celite pad, and upon concentration under reduced pressure, crude **9c** was obtained as oil. Column chromatography in 5% methanol/dichloromethane gave desired compound **9c** as colorless oil. (38 mg, 86%); ^{1}H NMR (400 MHz, $CDCl_3$) δ 6.68 (d, *J*=8.4 Hz, 1H), 6.56-6.49 (m, 2H), 3.73 (s, 3H), 3.54 (s, 2H), 2.55 (q, *J*=6.8 Hz, 4H), 1.03 (t, *J*=6.8, 6H); ^{13}C NMR (100 MHz, $CDCl_3$) δ 139.9, 117.8, 116.6, 114.0, 112.0, 110.6, 56.4, 51.0, 47.2, 11.9; ESI-MS (*m/z+1)* 209.[6]

Note: All structures in this section has suffix C.

General alkylation and *N*-alkylation Procedure.
The synthesis of compound **C3** (in main text **ICQ (13)**) and compounds **C6a-f** followed the general two-step synthetic pathway illustrated in Scheme 2.

General alkylation procedure. Previously has been reported that alkylation of potassium salt of phenols instead of phenols gives an overall better yields.[21] However, in our hands, direct alkylation of phenols (7-chloro-4-hydroxy quinoline (**C1**), 2,4-dichloro phenol (**C4a**) and 2-chloro-4-(trifluoromethyl) phenol (**C4f**)) afforded the intermediate compounds **C2** and **C5a-f** in quite satisfactory yields (45-70%); therefore we skipped the step of converting phenols to potassium salts.
Commercially available phenols **C1**, **C4a** and **C4f** (1.0 equiv) in the presence of base Li_2CO_3 (2 equiv) were dissolved in anhydrous 1-Methyl-2-pyrrolidinone (10 mL), and stirred under Argon atmosphere. 3 equiv. of corresponding *n*-dibromoalkane (*n*=2, 3, 4, 5, 6) was added and the reaction mixture was stirred for 16 h at 90°C. The reaction mixture was poured in 50 mL of water, and extracted with diethyl ether (3x35 mL). The organic layers were combined, dried over Na_2SO_4, filtered and evaporated to dryness.

General N-alkylation procedure. There are several available, high-yielding procedures describing *N*-alkylation of imidazoles reported to date[22]. However, during this reaction we observed the formation of unwanted side product- the quaternary imidazolium salt, which was not visible on LC-MS, but had similar Rf as target compounds. After some experimentation with other bases, we found that instead of using KOH, the equimolar amount of *N*, *N*-diisopropylethylamine in the presence of catalytic amount of tetrabutylammonium bromine in refluxing acetonitrile would provide compounds in moderate yields, 45-60%, with formation of unwanted quaternary imidazolium salts in limited amount.

The title compounds were prepared from intermediates described above following this general procedure: to a solution of corresponding intermediate (1 equiv), imidazole (2 equiv) and catalytic amount of TBAB (0.05 equiv) in anhydrous MeCN (15 mL) was added DIPEA (2 equiv) and then solution was refluxed overnight[23]. The solvent was evaporated and the crude mixture was suspended in water (25 mL) and organic materials were extracted with $CHCl_3$ (3 x 25 mL) and dried over Na_2SO_4. Upon filtration and evaporation of the solvent, the crude product was purified by column chromatography on silica gel with 5% methanol/dichloromethane.

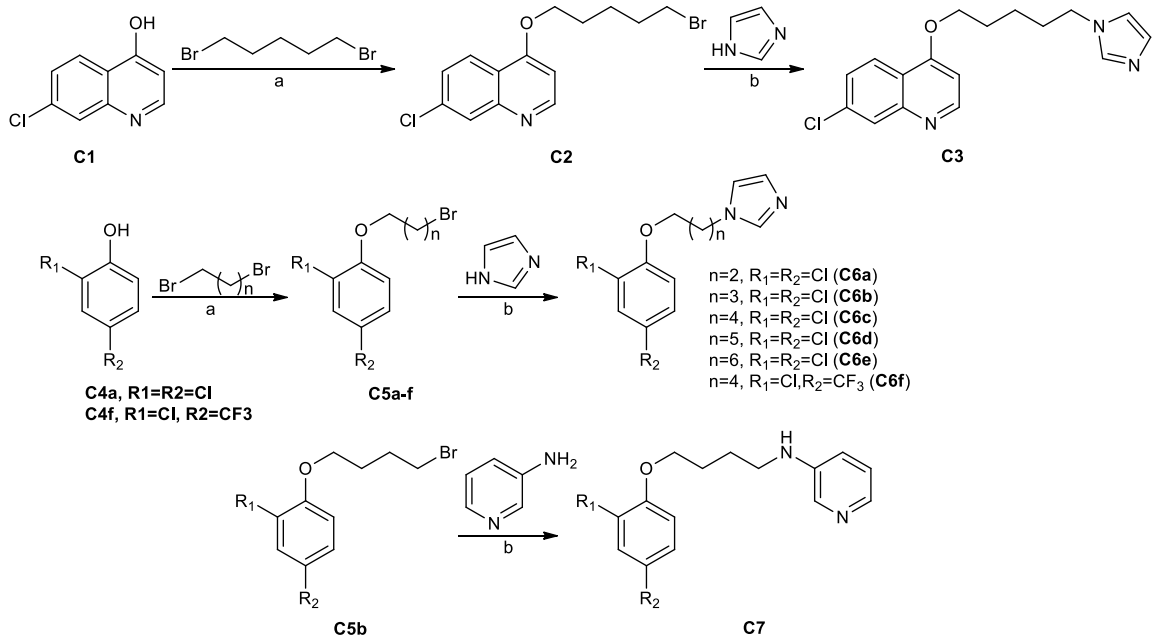

Scheme 2. *Reagents and conditions:* a) Li_2CO_3, NMP, 90°C, 16h; b) TBAB, DIPEA, MeCN, reflux, 12h.

4-((5-bromopentyl)oxy)-7-chloroquinoline, **C2**: Using general alkylation procedure, followed by chromatographic purification with 1:4 ethyl acetate:hexane solvent system as eluent, **C2** was afforded as a white solid (0.3 g, 24%). mp=63-65 °C. ^{1}H NMR ($CDCl_3$/Methanol-d_4, 9:1, 400 MHz): δ 8.56 (d, *J* = 11.2 Hz, 1H); 8.06 (d, *J* =12 Hz, 1H); 7.88 (d, *J* = 9.6 Hz, 1H); 7.35 (d, *J* = 9.2 Hz, 1H); 6.67 (dd, *J* =13.2 and 5.2 Hz, 1H); 4.12 (t, *J* = 6 Hz, 2H); 3.37 (t, *J* = 6 Hz, 2H); 1.90-1.85 (m, 4H); 1.66-1.60 (m, 2H). ^{13}C NMR ($CDCl_3$, 100 MHz): δ 162.0, 152.1, 148.8, 136.1, 126.7, 126.6, 123.5, 119.8, 100.9, 68.4, 33.3, 32.2, 27.8, 24.6. ESI-MS [m/z+H]: 328.

4-((5-(1H-imidazol-1-yl)pentyl)oxy)-7-chloroquinoline, **C3** (in main text **ICQ(13)**): The crude compound was purified by column chromatography in 10% methanol/dichloromethane solvent system to give **C3** as a colorless oil (0.55 g, 46%). ^{1}H NMR ($CDCl_3$, 400 MHz): δ 8.69 (d, *J* = 5.2 Hz, 1H); 8.06 (d, *J* =8.8 Hz, 1H); 8.00 (d, *J* = 2.4 Hz, 1H), 7.51 (s, 1H); 7.43 (dd, *J* =8.4 and 2 Hz, 1H); 7.06 (s, 1H); 6.91 (s, 1H); 6.67 (d, *J* = 5.2 Hz, 1H); 4.15 (t, *J* = 6 Hz, 4H); 3.99 (t, *J* = 7 Hz, 2H); 1.97-1.87 (m, 4H); 1.59-1.51 (m, 2H). ^{13}C NMR ($CDCl_3$, 100 MHz): δ 161.4, 152.4, 149.6, 136.9, 135.7, 129.3, 127.8, 126.5, 123.2, 119.7, 118.7, 100.8, 68.0, 46.8, 30.7, 28.3, 23.2. ESI-MS [m/z+H]: 316.

1-(3-bromopropoxy)-2,4-dichlorobenzene, C5a: The crude compound was purified by column chromatography in hexane to give **C5a** as a tan oil (0.585 g, 54%). ^{1}H NMR ($CDCl_3$, 400 MHz): δ 7.36 (d, *J* = 2.8 Hz, 1H); 7.18 (dd, *J* =8.8 and 2.8 Hz, 1H); 6.86 (d, *J* = 8.8 Hz, 1H); 4.14 (t, *J* = 6 Hz, 2H); 3.65 (t, *J* = 6 Hz, 2H); 2.35 (quin, *J* = 6 Hz, 2H). ^{13}C NMR ($CDCl_3$, 100 MHz): δ 153.1, 130.0, 127.7, 125.9, 123.8, 114.2, 66.8, 32.3, 30.0.

1-(4-bromobutoxy)-2,4-dichlorobenzene, C5b: The crude compound was purified by column chromatography in hexane to give **C5b** as colorless oil (0.685 g, 59%): ^{1}H NMR ($CDCl_3$, 400 MHz): δ 7.34 (d, *J* = 2 Hz, 1H); 7.15 (dd, *J* =8.4 and 2.4 Hz, 1H); 6.81 (d, *J* = 8.8 Hz, 1H); 4.02 (t, *J* = 6 Hz, 2H); 3.50 (t, *J* = 6 Hz, 2H); 2.11-1.96 (m, 4H). ^{13}C NMR ($CDCl_3$, 100 MHz): δ 153.1, 129.8, 127.5, 125.6, 123.6, 113.9, 68.3, 33.5, 29.4, 27.6.

1-((5-bromopentyl)oxy)-2,4-dichlorobenzene, C5c: The crude compound was purified by column chromatography in hexane to give **C5c** as colorless oil (0.725 g, 61%): ^{1}H NMR ($CDCl_3$, 400 MHz): δ 7.43 (d, *J* = 2.4 Hz, 1H); 7.24 (dd, *J* =8.8 and 2.8 Hz, 1H); 6.89 (d, *J* = 8.4 Hz, 1H); 4.07 (t, *J* = 6 Hz, 2H); 3.54 (t, *J* = 6.4 Hz, 2H); 2.06-1.92 (m, 4H); 1.78-1.72 (m, 2H). ^{13}C NMR ($CDCl_3$, 100 MHz): δ 153.2, 129.9, 127.4, 125.5, 123.6, 113.9, 69.0, 33.5, 32.3, 28.1, 24.7.

1-((6-bromohexyl)oxy)-2,4-dichlorobenzene, C5d: The crude compound was purified by column chromatography in hexane to give **C5d** as colorless oil (0.899 g, 72%): ^{1}H NMR ($CDCl_3$, 400 MHz): δ 7.33 (d, *J* = 2.8 Hz, 1H); 7.14 (dd, *J* =9.2 and 2.8 Hz, 1H); 6.80 (d, *J* = 8.4 Hz, 1H); 3.97 (t, *J* = 6 Hz, 2H); 3.39 (quin, *J* = 6.8 Hz, 2H); 1.90-1.80 (m, 4H); 1.53-1.45 (m, 4H). ^{13}C NMR ($CDCl_3$, 100 MHz): δ 153.3, 129.8, 127.4, 125.3, 123.6, 113.9, 69.1, 33.7, 32.6, 28.8, 27.8, 25.1.

1-((7-bromoheptyl)oxy)-2,4-dichlorobenzene, C5e: The crude compound was purified by column chromatography in hexane to give **C5e** as colorless oil (0.85 g, 65%): ^{1}H NMR ($CDCl_3$, 400 MHz): δ 7.31 (d, *J* = 2.8 Hz, 1H); 7.16 (dd, *J* =8.8 and 2.4 Hz, 1H); 6.78 (d, *J* = 9.2 Hz, 1H); 3.94 (t, *J* = 6 Hz, 2H); 3.38 (t, *J* = 6.8 Hz, 2H); 1.86-1.77 (m, 4H); 1.49-1.36 (m, 6H). ^{13}C NMR ($CDCl_3$, 100 MHz): δ 153.4, 129.9, 127.5, 125.4, 123.7, 114.0, 69.3, 33.9, 32.6, 28.9, 28.4, 28.0, 25.8.

1-((5-bromopentyl)oxy)-2-chloro-4-(trifluoromethyl)benzene, C5f: The crude compound was purified by column chromatography in hexane to give **C5f** as pale yellow oil (0.612 g, 46%): ^{1}H NMR ($CDCl_3$, 400 MHz): δ 7.56 (s, 1H); 7.40 (d, *J* =8.4 Hz, 1H); 6.89 (d, *J* = 8.4 Hz, 1H); 4.02 (s, 2H); 3.43-3.33 (m, 2H); 1.90-1.83 (m, 4H); 1.63-1.53 (m, 2H). ^{13}C NMR ($CDCl_3$, 100 MHz): δ 156.8, 127.3, 124.9, 123.1, 122.1, 112.4, 68.8, 33.3, 32.2, 27.9, 24.6.

1-(3-(2,4-dichlorophenoxy)propyl)-1H-imidazole, C6a: The crude compound was purified by column chromatography in 5% methanol/dichloromethane solvent system to give **C6a** as a colorless oil (0.30 g, 63%). ^{1}H NMR ($CDCl_3$, 400 MHz): δ 7.42 (s, 1H); 7.32 (d, *J* =2.4 Hz, 1H); 7.10 (dd, *J* =8.8 and 2.8 Hz, 1H); 6.99 (s, 1H); 6.87 (s, 1H); 6.71 (d, *J* = 9.2 Hz, 1H); 4.19 (t, *J* = 7 Hz, 2H); 3.84 (t, *J* = 6 Hz, 2H); 2.20 (quin, *J* = 6 Hz, 2H). ^{13}C NMR ($CDCl_3$, 100 MHz): δ 152.1, 137.2, 129.9, 129.5, 127.6, 126.1, 123.5, 118.8, 114.0, 64.8, 42.9, 30.4. ESI-MS: [m/z+H]: 271.

1-(4-(2,4-dichlorophenoxy)butyl)-1H-imidazole, C6b: The crude compound was purified by column chromatography in 5% methanol/dichloromethane solvent system to give **C6b** as a pale yellow oil (0.31 g, 62%). ^{1}H NMR ($CDCl_3$, 400 MHz): δ 7.43 (s, 1H); 7.28 (d, *J* =2.4 Hz, 1H); 7.09 (dd, *J* =9.2 and 2.8 Hz, 1H); 6.99 (s, 1H); 6.97 (s, 1H); 6.73 (d, *J* = 8.8 Hz, 1H); 3.99 (t, *J* = 7.2 Hz, 2H); 3.92 (t, *J* = 6 Hz, 2H); 1.95 (quin, *J* = 7.2 Hz, 2H), 1.76-1.71 (m, 2H). ^{13}C NMR ($CDCl_3$, 100 MHz): δ 153.0, 137.0, 129.9, 129.4, 127.5, 125.7, 123.5, 118.7, 113.9, 68.7, 46.6, 27.9, 25.8. ESI-MS: [m/z+H]: 285.

1-(5-(2,4-dichlorophenoxy)pentyl)-1H-imidazole, C6c (in main text **SP134 (15)**): The crude compound was purified by column chromatography in 5% methanol/dichloromethane solvent system to give **C6c** as a colorless viscous oil (0.25 g, 47%). ^{1}H NMR ($CDCl_3$, 400 MHz): δ 7.47 (s, 1H); 7.35 (d, *J* = 2 Hz, 1H); 7.15 (dd, *J* = 8.8 and 2.4 Hz, 1H); 7.05 (s, 1H); 6.91 (s, 1H); 6.79 (d, *J* = 8.4 Hz, 1H); 3.97 (t, *J* = 6.8 Hz, 2H); 1.91-1.81 (m, 4H); 1.55-1.49 (m, 2H). ^{13}C NMR ($CDCl_3$, 100 MHz): δ 153.4, 137.3, 130.2, 129.7, 127.7, 125.8, 123.8, 118.9, 114.1, 69.1, 47.1, 31.0, 28.7, 23.4. ESI-MS: [m/z+H]: 299.

1-(6-(2,4-dichlorophenoxy)hexyl)-1H-imidazole, C6d: The crude compound was purified by column chromatography in 5% methanol/dichloromethane solvent system to give **C6d** as a colorless oil (0.25 g, 51%). ^{1}H NMR ($CDCl_3$, 400 MHz): δ 7.43 (s, 1H); 7.32 (d, *J* = 2.4 Hz, 1H); 7.13 (dd, *J* = 8.8 and 2.4 Hz, 1H); 7.02 (s, 1H); 6.87 (s, 1H); 6.78 (d, *J* = 8.8 Hz, 1H); 3.93 (quin, *J* = 6.4 Hz, 4H); 1.83-1.75 (m, 4H); 1.54-1.47 (m, 2H); 1.38-1.32 (m, 2H). ^{13}C NMR ($CDCl_3$, 100 MHz): δ 153.2, 136.9, 129.8, 129.1, 127.4, 125.4, 123.5, 118. 6, 113.8, 68.9, 46.7, 30.8, 38.6, 26.0, 25.4. ESI-MS: [m/z+H]: 313.

1-(7-(2,4-dichlorophenoxy)heptyl)-1H-imidazole, C6e: The crude compound was purified by column chromatography in 5% methanol/dichloromethane solvent system to give **C6e** as a colorless viscous oil (0.3 g, 53%). ^{1}H NMR ($CDCl_3$, 400 MHz): δ 7.54 (s, 1H); 7.43 (d, *J* = 0.8 Hz, 1H); 7.24 (dd, *J* = 8.4 and 0.8 Hz, 1H); 7.14 (s, 1H); 6.98 (s, 1H); 6.90 (d, *J* = 9.2 Hz, 1H); 4.06 (t, *J* = 6 Hz, 2H); 4.01 (t, *J* = 7.2 Hz, 2H); 1.92-1.86 (m, 4H); 1.59-1.41 (m, 6H). ^{13}C NMR ($CDCl_3$,

100 MHz): δ 153.4, 137.0, 129.9, 129.3, 127.5, 125.4, 123.6, 118.7, 114.0, 69.2, 46.9, 30.9, 28.8, 28.7, 26.4, 25.8. ESI-MS: [m/z+H]: 327.

1-(5-(2-chloro-4-(trifluoromethyl)phenoxy)pentyl)-1H-imidazole, C6f: The crude compound was purified by column chromatography in 5% methanol/dichloromethane solvent system to give **C6f** as a colorless oil (0.23 g, 40%). ^{1}H NMR ($CDCl_3$, 400 MHz): δ 7.69 (s, 1H); 7.54 (s, 1H); 7.52 (s, 1H), 7.12 (s, 1H); 7.01 (s, 1H); 6.99 (s, 1H); 4.12 (t, *J* = 6 Hz, 2H); 4.05 (t, *J* = 7.2 Hz, 2H); 1.97-1.92 (m, 4H); 1.61-1.58 (m, 2H). ^{13}C NMR ($CDCl_3$, 100 MHz): δ 156.9, 137.1, 129.5, 127.5, 125.1, 123.6, 123.3, 122.3, 118.8, 112.5, 68.9, 46.9, 30.8, 28.4, 23.3. ESI-MS: [m/z+H]:333.

N-(4-(2,4-dichlorophenoxy)butyl)pyridin-3-amine, C7 (in main text **SP148 (14)):** The crude compound was purified by column chromatography in 0-5% methanol/dichloromethane solvent system to give **10** as a colorless viscous oil (0.029 g, 35%). ^{1}H NMR ($CDCl_3$, 400 MHz): δ 8.10 (s, 1H); 7.91 (d, *J* = 7.2 Hz, 1H); 7.35 (s, 1H), 7.15 (dd, *J* = 10.4 and 2.8 Hz, 2H); 6.93 (d, *J* = 8.4 Hz, 1H); 6.82 (d, *J* = 8.4 Hz, 1H); 4.05 (t, *J* = 5.6 Hz, 2H); 3.24 (t, *J* = 6.4 Hz, 2H); 1.96 (t, *J* = 6.8 Hz, 2H); 1.89 (t, *J* = 6.8 Hz, 2H); 1.24 (bs, 1H). ^{13}C NMR ($CDCl_3$, 100 MHz): δ 153.3, 144.8, 136.8, 134.7, 130.1, 127.7, 124.3, 119.3, 114.0, 114.0, 69.1, 43.2, 26.6, 26.0. ESI-MS: [m/z+H]:311.

General synthesis of amide quinolines procedure.
General route for synthesis of amide quinoline derivatives is shown in Scheme 3 below. A commercially available 2-(4-bromo-phenyl) quinoline-4-carboxylic acid **C8** was activated by 1,1-carbonyldiimidazole and the appropriate *n*-aminoalkyl imidazole (n=2, 3 or 4) was added to obtain the target structures **C9a-d**. These conversions provided the desired derivatives in good yields and all target compounds were isolated either as crystalline solids, or we converted them into suitable salts. These set of analogs with simple modifications in length of linker between imidazole ring and the amide bond would allow us to examine the effects of increased or decreased lipophilicity of these structures on reactivation activity.

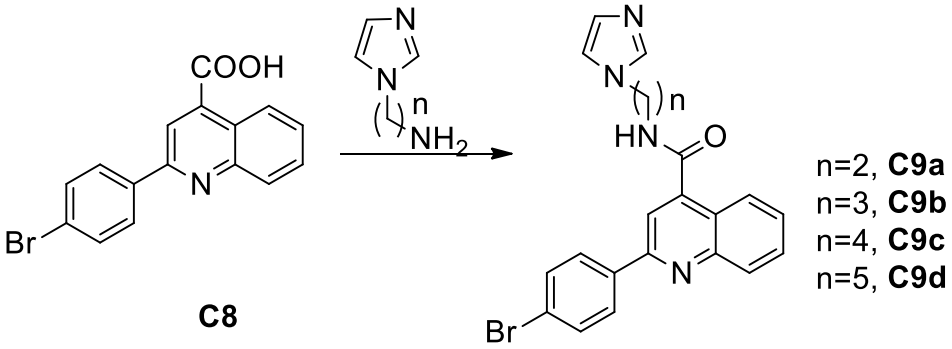

Scheme 3. *Reagents and conditions*: CDI, THF, rt, 12 h, reflux, 5h.

General procedure for the preparation of compounds **C9a-d**: A mixture of 2.75 mmol of the carboxylic acid **C8** and 3.025 mmol of 1,1'-carbonyldiimidazole in 15 mL of THF was stirred at room temperature for 1.5 h. The reaction mixture was cooled to 0°C and 2.75 mmol of the appropriate *n*-aminoalkyl imidazole (n=2,3,4) was added. The reaction mixture was then stirred at room temperature for 18-24 h, and refluxed for 5 h. The solvent was removed in vacuo and the residue was dissolved in 20 mL of diethyl ether and treated with 1N HCl. Acid layer was separated, basified with saturated $NaHCO_3$, and extracted with ethyl acetate (3x25 mL). The organic layers were combined, dried over Na_2SO_4, and concentrated to give the desired crude product.

N-(2-(1H-imidazol-1-yl)ethyl)-2-(4-bromophenyl)quinoline-4-carboxamide, **C9a**: The crude compound was purified by column chromatography in 5% methanol/dichloromethane solvent system to give **C9a** as a pale yellow solid (0.82 g, 71%). ^{1}H NMR (Methanol-d_4, 400 MHz): δ 8.11 (t, *J* = 8.4 Hz, 3H); 7.96 (d, *J* = 8 Hz, 2H); 7.88 (s, 1H); 7.79 (t, *J* = 7.2 Hz, 1H); 7.71 (d, *J* = 8.4 Hz, 2H); 7.60 (t, *J* = 7.2 Hz, 1H); 7.35 (s, 1H); 7.15 (s, 1H); 4.38 (d, *J* = 5.2 Hz, 2H); 3.89 (d, *J* =

5.6 Hz, 2H). ^{13}C NMR (Methanol-d_4, 100 MHz): δ 170.2, 156.9, 149.6, 144.3, 139.0, 133.1, 131.6, 130.6, 130.3, 128.6, 126.2, 125.4, 124.6, 117.7, 47.4, 41.3. ESI-MS: [m/z+H]: 421.

N-(3-(1H-imidazol-1-yl)propyl)-2-(4-bromophenyl)quinoline-4-carboxamide, **C9b** (in main text **SP138 (16)**): The crude compound was purified by column chromatography in 5% methanol/dichloromethane solvent system to give **C9b** as a yellow solid (0.84 g, 69%). ^{1}H NMR ($CDCl_3$, 400 MHz): δ 8.06 (s, 1H); 7.95 (d, *J* = 8.8 Hz, 1H); 7.79 (d, *J* = 7.6 Hz, 2H); 7.57 (d, *J* = 8.8 Hz, 2H); 7.45 (d, *J* = 8 Hz, 2H); 7.37 (t, *J* = 7.6 Hz, 1H); 7.13 (s, 1H); 6.75 (t, *J* = 15 Hz, 2H); 3.83 (t, *J* = 6.4 Hz, 2H); 3.26 (d, *J* = 8 Hz, 2H); 1.92 (t, *J* = 6.8 Hz, 2H). ^{13}C NMR ($CDCl_3$, 100 MHz): δ 167.9, 155.3, 148.6, 142.6, 137.5, 136.9, 132.0, 130.4, 130.0, 129.3, 128.9, 127.5, 124.9, 124.4, 123.4, 118.9, 116.1, 44.7, 37.3, 30.9. ESI-MS: [m/z+H]: 436.

N-(4-(1H-imidazol-1-yl)butyl)-2-(4-bromophenyl)quinoline-4-carboxamide, **C9c**: The crude compound was purified by column chromatography in 5% methanol/dichloromethane solvent system to give **C9c** as a colorless oil (0.75 g, 61%). ^{1}H NMR ($CDCl_3$, 400 MHz): δ 8.08 (s, 1H); 8.00 (d, *J* = 8 Hz, 2H); 7.83 (d, *J* = 8 Hz, 2H); 7.64 (t, *J* = 6.4 Hz, 2H); 7.51 (d, *J* = 7.6 Hz, 2H); 7.43 (t, *J* = 7.6 Hz, 1H); 7.11 (s, 1H); 6.77 (d, *J* = 6.8 Hz, 2H); 3.80 (t, *J* = 6.8 Hz, 2H); 3.36 (t, *J* = 6.8 Hz, 2H); 1.69 (t, *J* = 7.2 Hz, 2H); 1.45 (t, *J* = 7.6 Hz, 2H). ^{13}C NMR ($CDCl_3$, 100 MHz): δ 167.5, 154.9, 148.1, 142.7, 137.2, 136.4, 131.7, 130.0, 129.6, 128.7, 128.6, 127.1, 124.8, 124.8, 124.1, 123.2, 118.6, 115.9, 46.2, 38.8, 28.1, 26.2. ESI-MS: [m/z+H]: 449.

N-(5-(1H-imidazol-1-yl)pentyl)-2-(4-bromophenyl)quinoline-4-carboxamide, **C9d**: The crude compound was purified by column chromatography in 5% methanol/dichloromethane solvent system to give **C9d** as a tan oil (0.85 g, 67%). ^{1}H NMR ($CDCl_3$, 400 MHz): δ 8.08 (dd, *J* = 12.8 and 8.8 Hz, 2H); 7.96 (d, *J* = 10.4 Hz, 2H); 7.72 (dd, *J* = 13.6 and 5.6 Hz, 2 H); 7.60 (d, *J* = 8.4 Hz, 2H); 7.52 (t, *J* = 7.6 Hz, 1H), 7.33 (s, 1H), 6.96 (d, *J* = 16.8 Hz, 2H), 6.85 (s, 1H); 3.88 (t, *J* = 6.8 Hz, 2H); 3.46 (dd, *J* = 13.2 and 6.8 Hz, 2H); 1.79 (t, *J* = 7.6 Hz, 2H); 1.64 (t, *J* = 7.2 Hz, 2H); 1.34 (t, *J* = 7.6 Hz, 2H). ^{13}C NMR ($CDCl_3$, 100 MHz): δ 167.7, 155.4, 148.6, 143.2, 137.7, 137.0, 132.1, 130.4, 130.1, 129.2, 129.0, 127.5, 125.1, 124.5, 123.5, 118.9, 116.1, 46.9, 39.8, 30.6, 29.2, 24.0. ESI-MS: [m/z+H]: 463.

Synthesis of Sarin and Soman Safe Analogs.

Safety Warning. Sarin and Soman Safe Analogs are also anticholinesterases and must be handled with care; rubber gloves must be worn and glassware decontaminated in 2M aqueous NaOH.

Procedure for the preparation of Sarin Safe Analog: Methylphosphonic dichloride (1.48 g, 11.14 mmol) and 4-nitrophenol (1.29 g, 9.3 mmol) were stirred in diethyl ether (75 ml) at room temperature for 15 minutes under argon atmosphere. Reaction mixture was cooled to 0°C and triethylamine (1.29 ml, 9.3 mmol) in diethyl ether (25 ml) was added slowly and the mixture was stirred at room temperature overnight. 2-propanol (1.42 mL, 18.56 mmol) and triethylamine (2.6 mL, 18.56 mmol) in diethyl ether (25 ml) were added slowly and the mixture was stirred at room temperature for an additional 4 h. The reaction mixture was filtered and washed with 1% aqueous sodium bicarbonate (become greenish). The organic phase was dried over anhydrous sodium sulfate and evaporated on a rotary evaporator. The yellow liquid product was dissolved in hot hexane and left in refrigerator (-20°C) overnight. Purification was done in 1:1 ethyl acetate:hexane solvent system, obtaining Sarin Safe Analog as a pale yellow liquid.[24]

Isopropyl (4-nitrophenyl) methylphosphonate (**NIMP**, in main text **11**). ^{1}H NMR ($CDCl_3$, 400 MHz): δ 8.23 (d, *J* = 7.2 Hz, 2H), 7.38 (d, *J* = 8.4 Hz, 2H), 4.82 (t, *J* = 6.4 Hz, 1H), 1.67 (d, *J* = 19.6 Hz, 3H), 1.36 (d, *J* = 7.6 Hz, 3H); 1.27 (d, *J* = 8 Hz, 3H). ^{13}C NMR ($CDCl_3$, 100 MHz): δ 155.9, 144.1, 125.7, 121.0, 72.2, 24.1, 23.9, 13.2.

Procedure for the preparation of Soman Safe Analog: The procedure was the same as described above for NIMP, except that instead of 2-propanol, pinacolyl alcohol was used. Purification was

done first in 100% hexane to remove excess pinacolyl alcohol and then it was switched to 1:1 ethyl acetate:hexane in order to collect final compound as a pale green liquid.

3,3-dimethylbutan-2-yl (4-nitrophenyl) methylphosphonate (**SIMP**, in main text **11a**) – *Diastereomeric pair*. ^{1}H NMR ($CDCl_3$, 400 MHz): δ 8.16 (d, *J* = 5.2 Hz, 2H), 8.13 (d, *J* = 5.2 Hz, 2H), 6.92 (d, *J* = 5.2 Hz, 2H), 6.89 (d, *J* = 5.2 Hz, 2H), 4.42-4.34 (m, 2H), 1.74 (d, *J* = 2 Hz, 3H), 1.69 (d, *J* = 2 Hz, 3H), 1.34 (d, *J* = 6.4 Hz, 3H), 1.18 (d, *J* = 6 Hz, 3H), 0.94 (s, 9H), 0.88 (s, 9H). ^{13}C NMR ($CDCl_3$, 100 MHz): δ 162.0, 141.6, 126.3, 125.8, 115.7, 84.0, 83.6, 35.2, 35.1, 25.6, 17.1, 13.5, 12.6, 12.0, 11.2.

Supplementary Figures

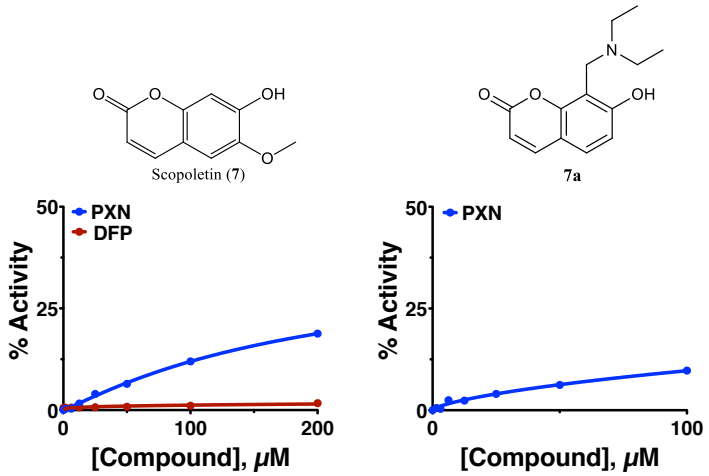

Figure S2. Reactivation of huAChE by other phenols, scopoletin (7) and 7a. Scopoletin (**7**) (left) and related analog **7a** (right) were able to reactivate paraoxon, PXN (**1**) adducts (blue) to an appreciable degree. Reactivation of **DFP** (**2**) adducts (red) by scopoletin (**7**) was not significant. Reactivation was measured in solution phase and is expressed in % activity relative to the uninhibited enzyme.

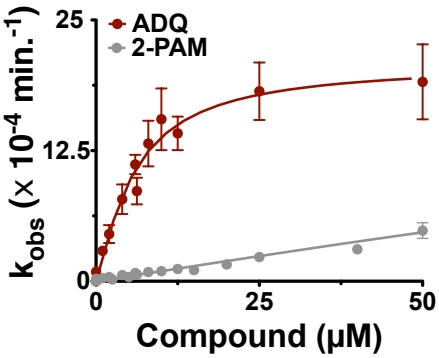

Figure S3. Reactivation of DFP (2)-inhibited huAChE by ADQ (**6**)**.** Dependence of the reactivation rate constant on the concentration of **ADQ** (**6**) in red or pralidoxime (**5**) in gray for **DFP** (**2**)-inhibited human AChE. Assay details can be found in the Experimental Section.

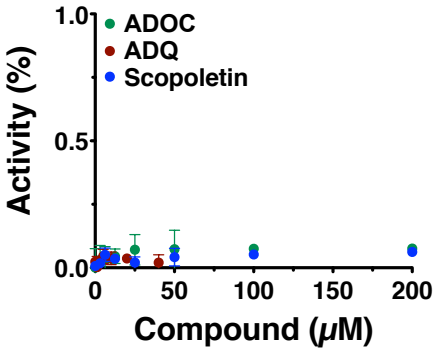

Figure S4. Background signal due to reactivator. The indicated concentrations of reactivator was added to ATCh and DTNB (2mM) to monitor how much reactivation is due to background ATCh hydrolysis by the reactivator itself. These controls were run at the same time and under identical conditions to the reactivation assays shown in the main text.

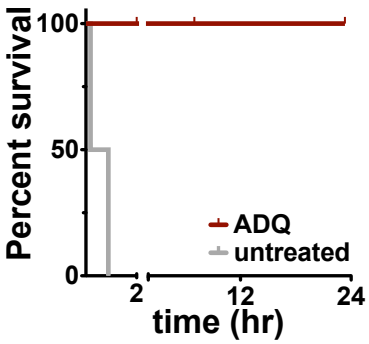

Figure S5. ADQ (6) protects animals from a lethal dose of DFP (2). Three animals were fed 5mg of **ADQ** (**6**) prior to challenge with an otherwise lethal dose (3mg/kg). All the animals treated with **ADQ** (**6**) survived (3), whereas the untreated animals (2) expired within 50 min.

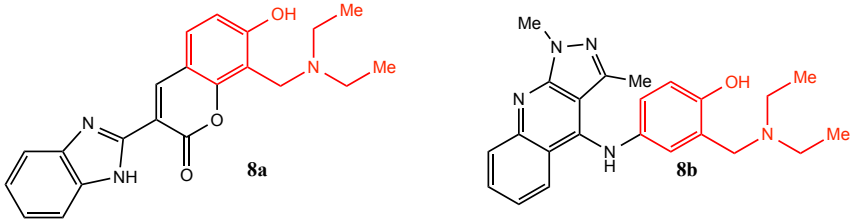

Figure S6. Mannich phenol containing hits. Many hits from our screening efforts contained the same functional group and we examined the activity of related compounds. Activity is shown in Figure S7.

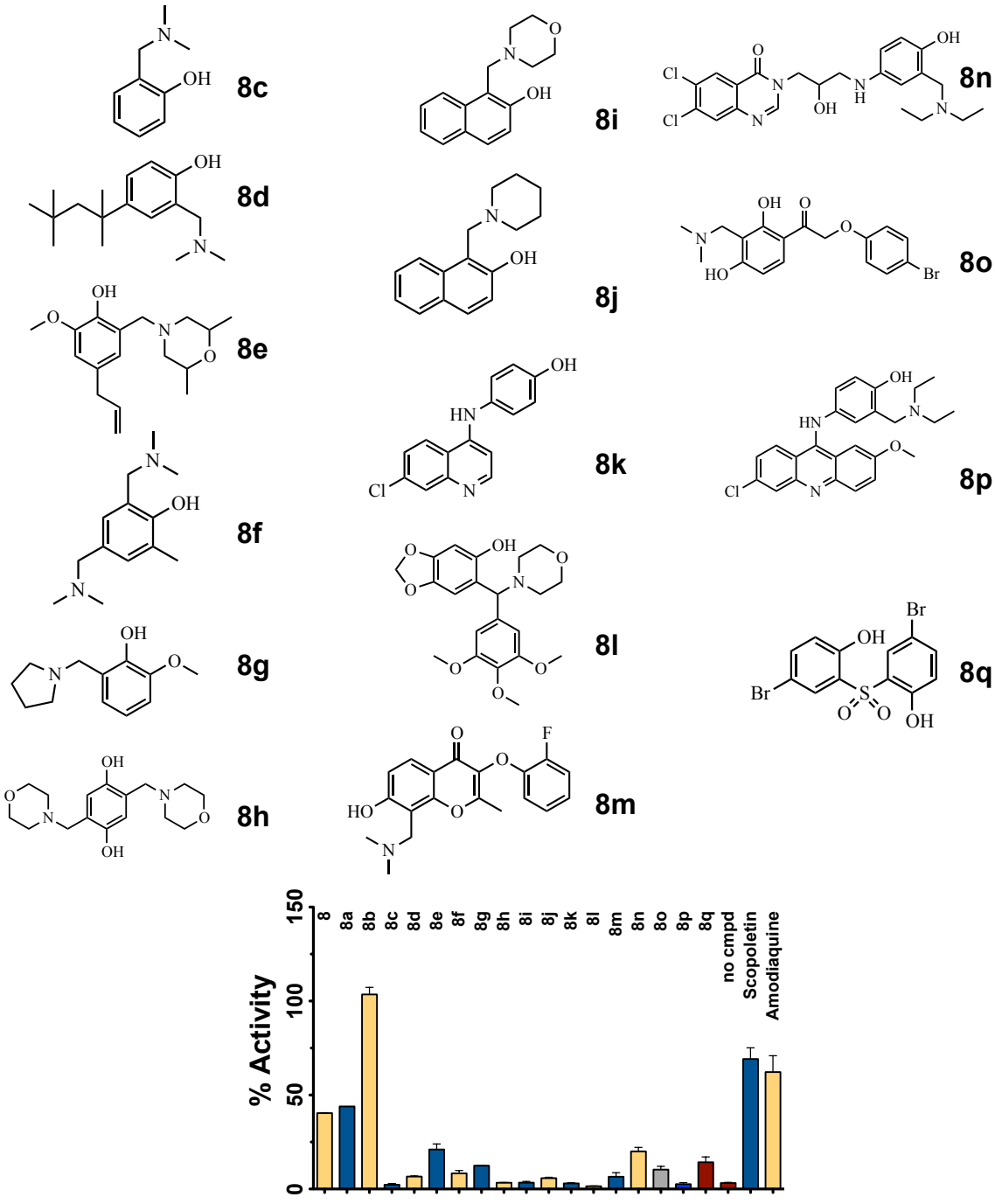

Figure S7. Alternate phenol containing compounds for additional screening. A variety of compounds containing phenol groups were tested for reactivation activity. Activity was measured in our screening format on solid phase and is expressed at % activity relative to an uninhibited control (fully active), and any compounds with significant activity were confirmed with dose-response curves in solution phase.

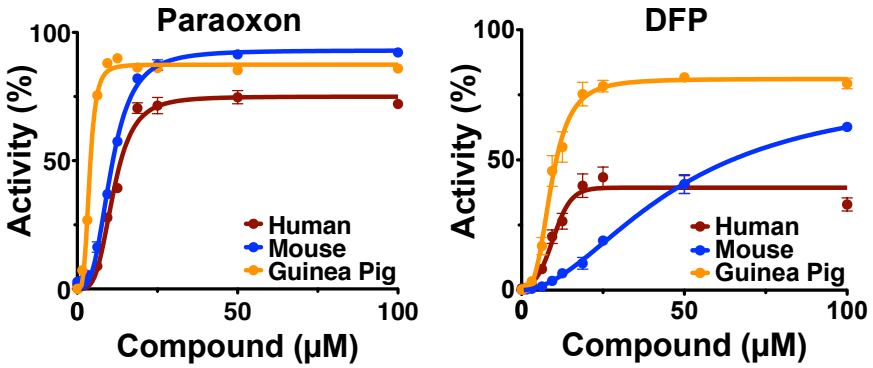

Figure S8. Reactivation of paraoxon (1) or DFP (2) inhibited AChE by ADOC (9). Increasing concentrations of **ADOC** (**9**) were added to paraoxon (**1**) (left) or **DFP** (**2**) (right)-inhibited human (red), mouse (blue), and guinea pig forms (orange) of AChE. At concentrations above 25μM, **ADOC** (**9**) reactivates all forms of the paraoxon (**1**)-inhibited enzyme to near completion. Reactivation is expressed in terms of % activity relative to uninhibited, untreated enzyme.

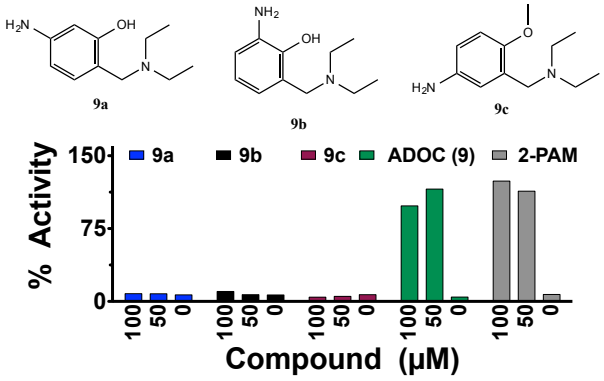

Figure S9. Analogs of ADOC (9). We synthesized the meta- (**9a**) and ortho- (**9b**) analogs of **ADOC (9)** and an analog with a blocked phenol group (**9c**). Results from solution phase activity assays showed that analogs of **ADOC** (**9**) were not active at reactivation of muAChE inhibited with paraoxon (**1**).

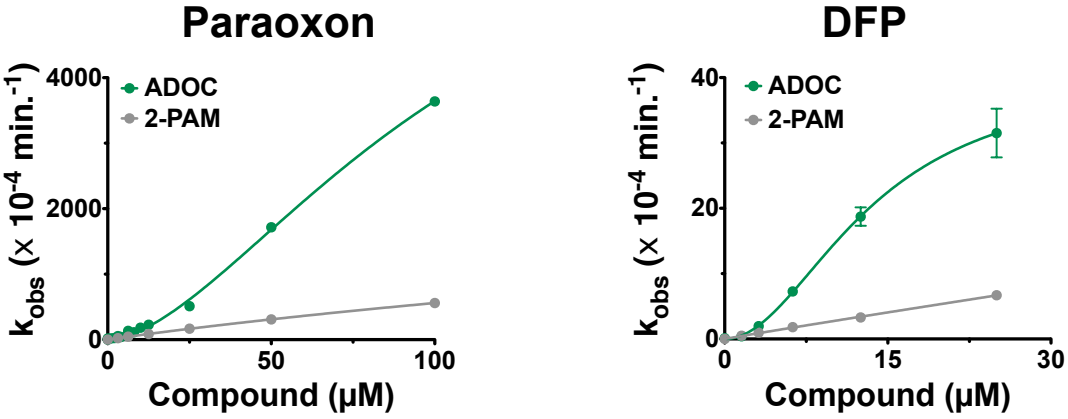

Figure S10. Concentration dependence of reactivation rate constants for reactivation of mouse AChE by ADOC (9). Reactivation by **ADOC** (**9**) (green) of the mouse form of AChE was much faster at lower concentrations than pralidoxime (**5**) (gray) and was best fit to an allosteric model of kinetics, with a Hill coefficient of 1.7 +/- 0.11 for paraoxon (**1**) and 2.0 +/- 0.3 for **DFP** (**2**). Maximum rate of reactivation was achieved at concentrations much lower than for pralidoxime (**5**).

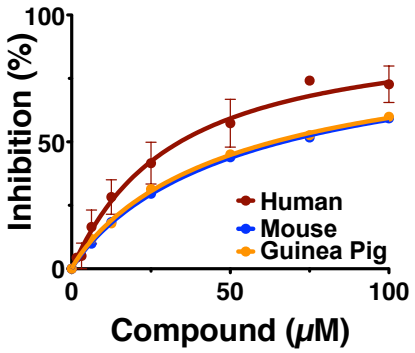

Figure S11. Inhibition of huAChE by ADOC (9). Full Michaelis-Menten kinetics was measured at increasing concentrations of **ADOC (9)** in order to calculate V_{max}. The V_{max} in the presence of the indicated concentrations of **ADOC (9)** was set relative to the V_{max} in its absence of **ADOC (9),** converted to % by multiplying by 100 (% activity relative to the V_{max} of fully active form), and then subtracted from 100 in order to plot as % inhibition.

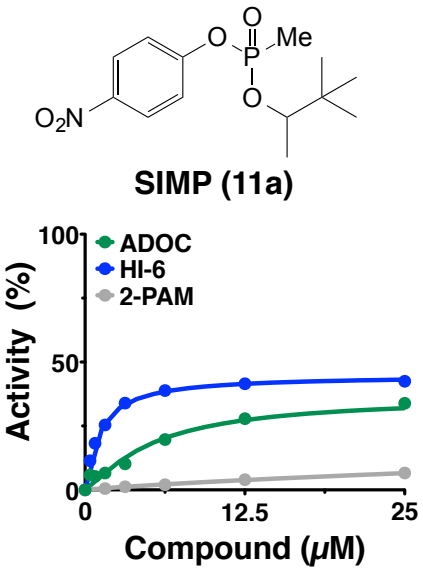

Figure S12. Reactivation of SIMP (11a) inhibited AChE. SIMP (**11a**) is safer to handle than soman (**4**), yet it creates the same adduct as soman (**4**) at the active site of AChE. Soman (**4**) and **SIMP** (**11a**) are composed of different diasteromers, which have different rates of inhibition and reactivation when they react with AChE. Because the leaving group of **SIMP** (**11a**) is different from that of soman (**4**) (nitrophenol vs. fluoride), there may be a difference in the ratio of isomeric adducts that form, such that the isomeric form that results more frequently from **SIMP** (**11a**) inhibition may be easier to reactivate than that formed after soman (**4**) inhibition. AChE that had been inhibited with **SIMP** (**11a**) was treated with reactivation compound immediately after isolation from excess **SIMP** (**11a**) using a PD10 column, to reduce the possibility of forming an aged adduct. Comparison of the reactivation of **SIMP** (**11a**)-huAChE by **HI-6** (**10**) (blue), pralidoxime (**5**) (gray), and **ADOC** (**9**) (green), reactivation by **ADOC** (**9**) and **HI-6** (**10**) was similar at the highest concentrations after 3 hrs of incubation.

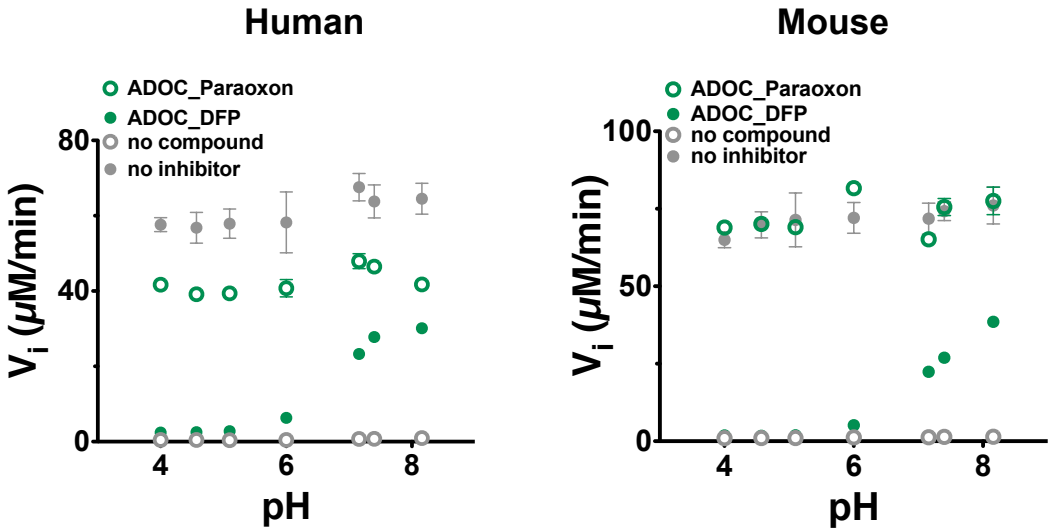

Figure S13. pH dependence of reactivation. Reactivation of either paraoxon (**1**) (open green circles) or **DFP** (**2**) (closed green circles) inhibited AChE (human enzyme on the left, and mouse enzyme on the right) by **ADOC** (**9**) was carried out at the indicated pHs, before adding to standard pH 7.4 phosphate buffer and measuring breakdown of acetylthiolcholine. Controls showing full activity (no OPC added) are shown in the gray solid circles, whereas activity in the absence of **ADOC** (**9**) (i.e. spontaneous reactivation) is shown with open gray circles. Initial rates are expressed in terms of μM product generated per minute. We express activity this way here to show that the initial rate did not vary much with pH.

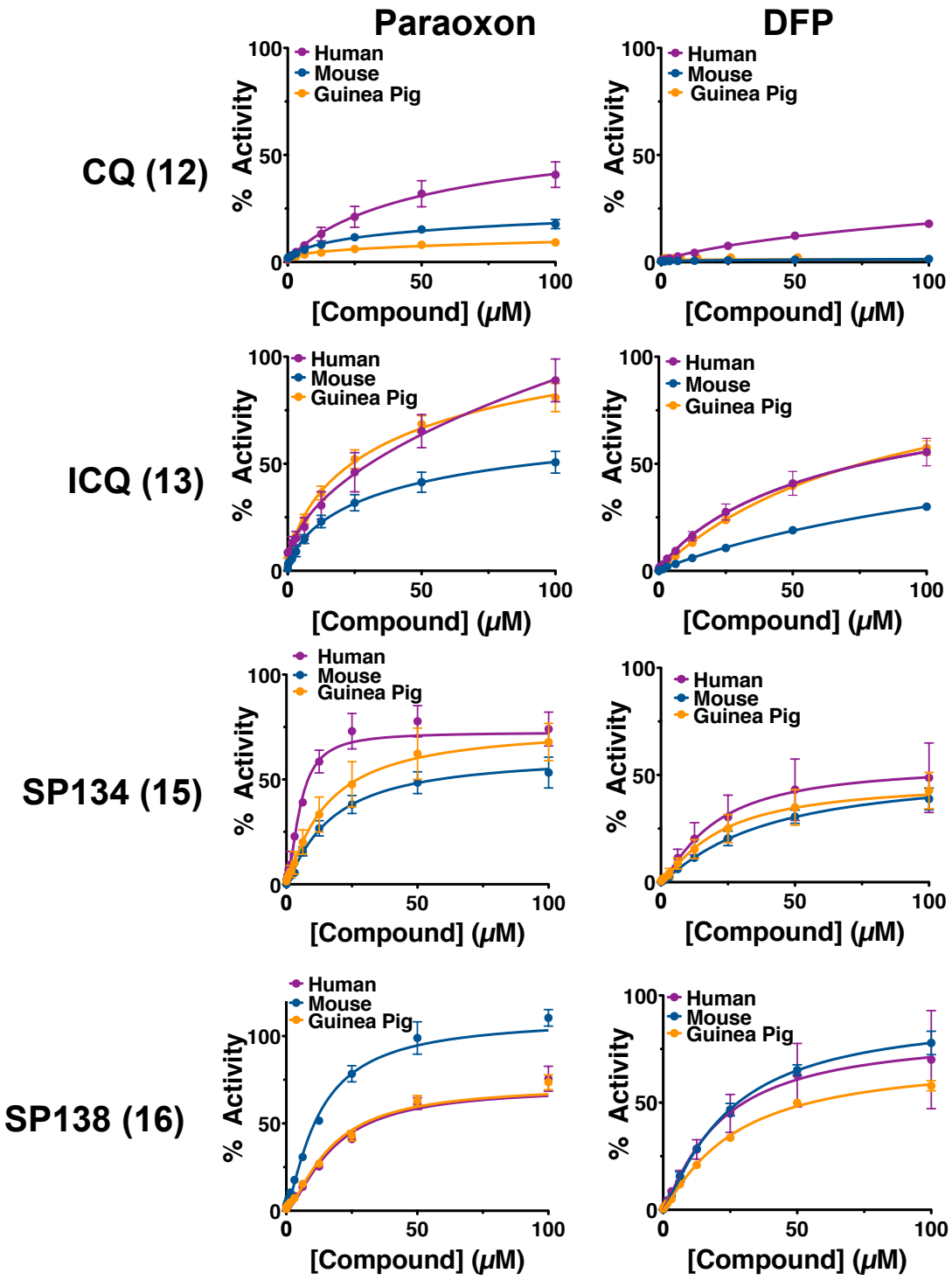

Figure S14. Concentration dependence of newly identified reactivators of OPC-inhibited AChE. Reactivation by **CQ** (**12**), **ICQ** (**13**), **SP134** (**15**) or **SP138** (**16**) of AChE from different species (human, plum; mouse, blue; guinea pig, orange) was tested using our solution phase assay, followed by dilution. Reactivation of **DFP** (**2**)-inhibited human enzyme was allowed to proceed overnight, whereas in all other cases, reactivation was measured after 3 hrs.

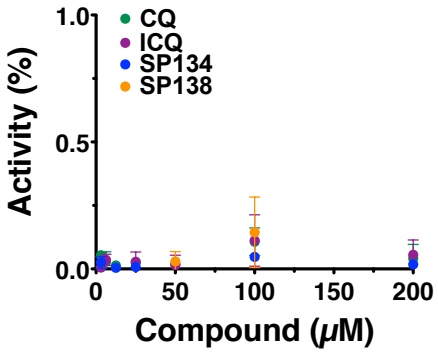

Figure S15. Background signal due to reactivation compound. In order to ensure the signal from ATCh hydrolysis was due to enzyme activity and not background hydrolysis, the indicated concentrations of reactivator was added to ATCh and DTNB (2mM) in the absence of enzyme. These reactions were run in parallel to the reactivation assays in the main text and were run under identical conditions to those described.

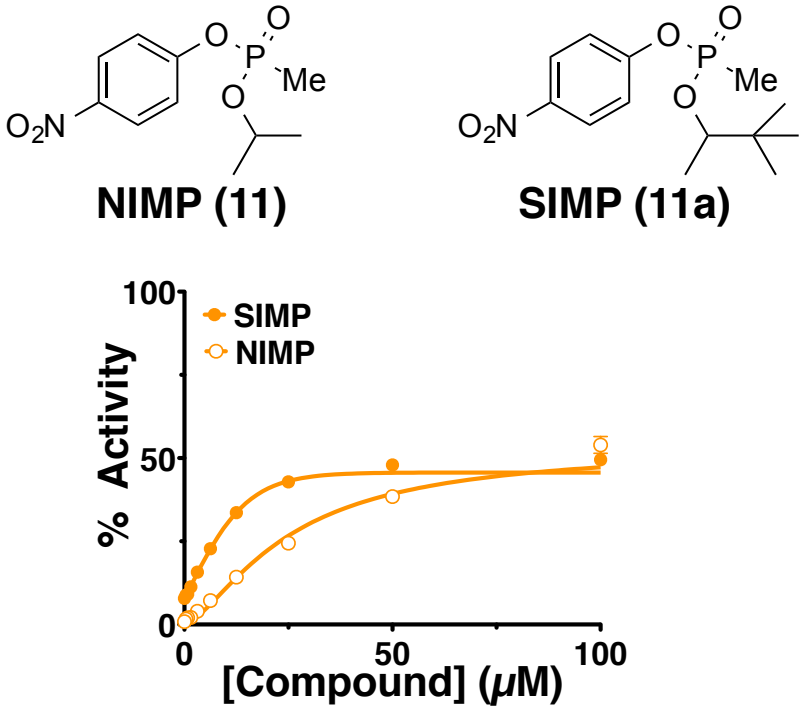

Figure S16. Concentration dependence of reactivation of NIMP (11) and SIMP (11a) inhibited AChE by SP138 (16). We synthesized nerve agent analogs, **NIMP** (**11**) and **SIMP** (**11a**), which leave the same adducts as sarin (**3**) and soman (**4**) in the AChE active site. Note that soman (**4**) and **SIMP** (**11a**) are composed of different diasteromers, which have different rates of inhibition and reactivation when they react with AChE. Because the leaving group of **SIMP** (**11a**) is different from that of soman (**4**) (nitrophenol vs. fluoride), there may be a difference in the ratio of isomeric adducts that form, such that the isomeric form that results more frequently from **SIMP** (**11a**) inhibition may be easier to reactivate than that formed after soman (**4**) inhibition. In order to avoid complications due to potential aging, the reactivator was added as quickly as possibly to the inhibited-AChE after removal of excess OPC. Reactivation at the indicated concentrations of **SP138** (**16**) of huAChE that was inhibited by **NIMP** (**11**) (open circles) or **SIMP** (**11a**) (closed circles). Reactivation was allowed 3 hrs for completion.

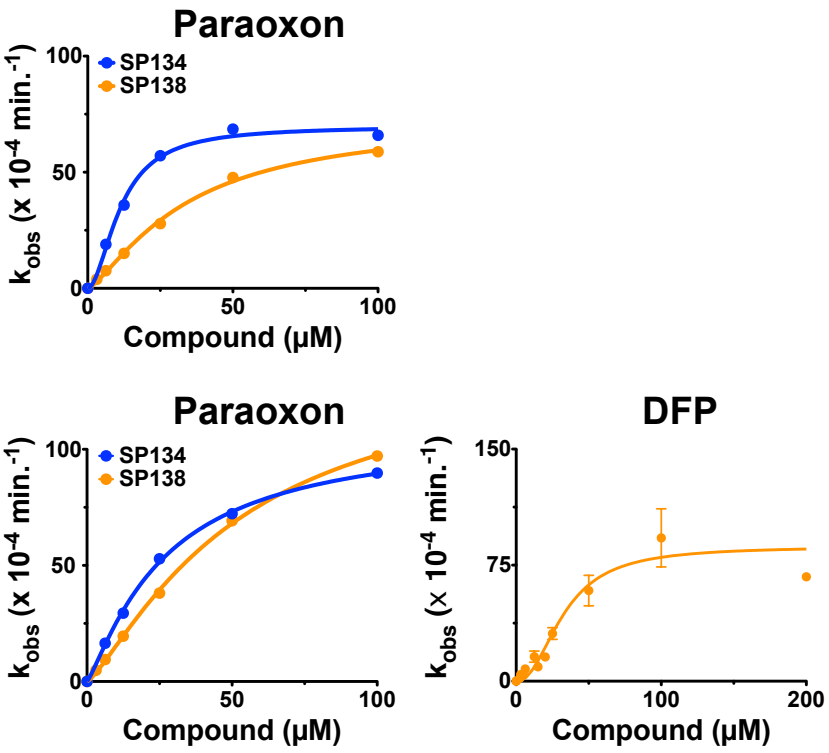

Figure S17. Concentration dependence of reactivation by SP134 (15) or SP138 (16). Reactivation by **SP134** (**15**) (blue), **SP138** (**16**) (orange) of recombinant human AChE inhibited by paraoxon (**1**) (top) or mouse AChE (bottom) inhibited by paraoxon (**1**) (left) or **DFP** (**2**) (right). Reactivation by **SP134** (**15**) of mouse enzyme inhibited by **DFP** (**2**) is shown in the body of the paper. The kinetic parameters determined can be found in Table S1.

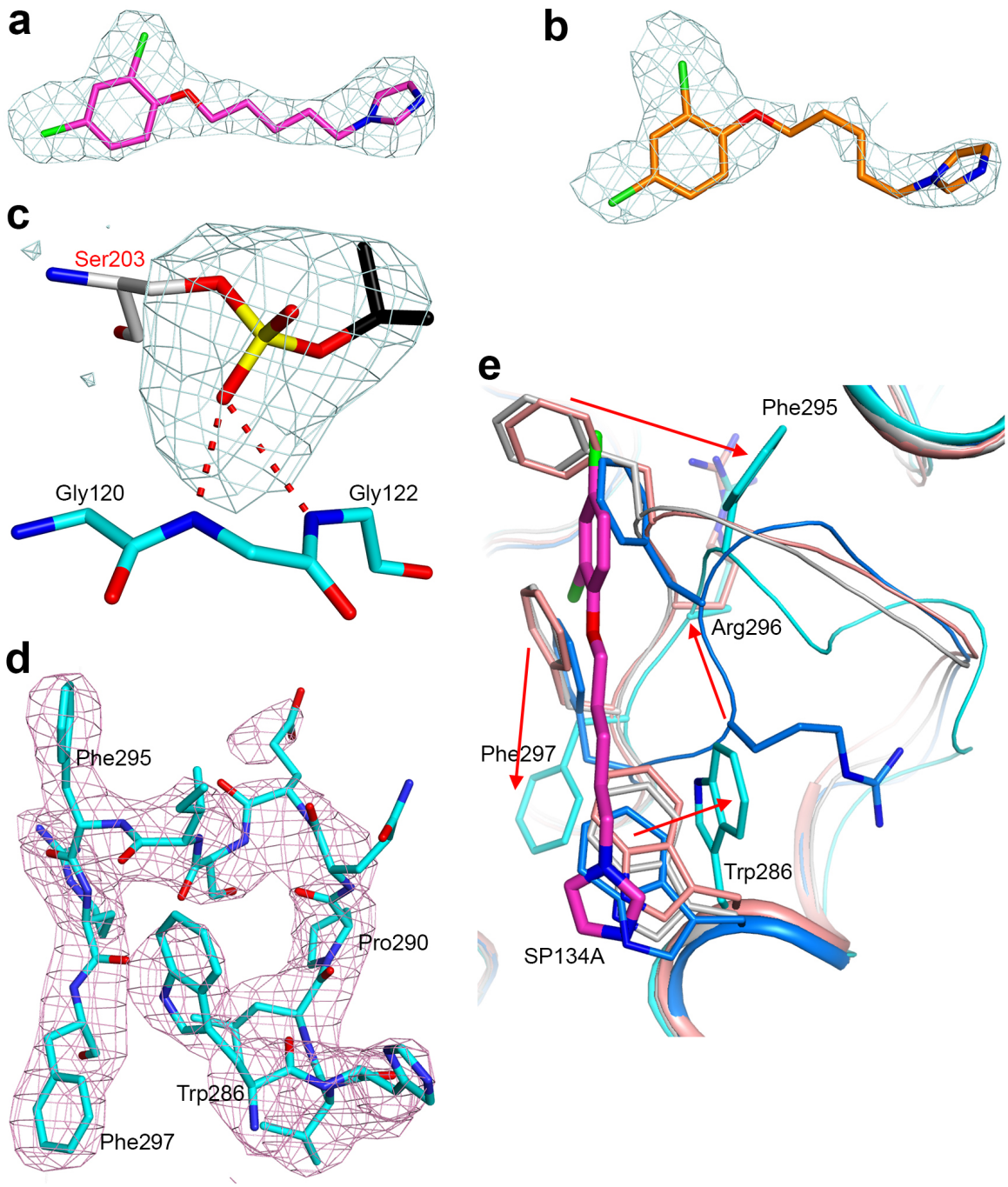

Figure S18. Additional structural comparisons. Omit F_o–F_c electron density at 2.7 Å resolution for a) **SP134**A; b) **SP134**B; c) **DFP** (**2**) group on the catalytic Ser203; and d) the segment containing residues 286-297, contoured at 2.5σ. e) Overlay of the structures of the segment containing residues 286-297 of murine AChE in complex with **SP134** (**15**) (cyan for AChE and magenta for **SP134**A), **DFP** (**2**)-modified murine AChE (gray), *Torpedo californica* AChE alone (salmon), and aged **DFP** (**2**)-modified *Torpedo californica* AChE (marine). Large conformational differences for the three aromatic residues and Arg296 are indicated with the red arrows.

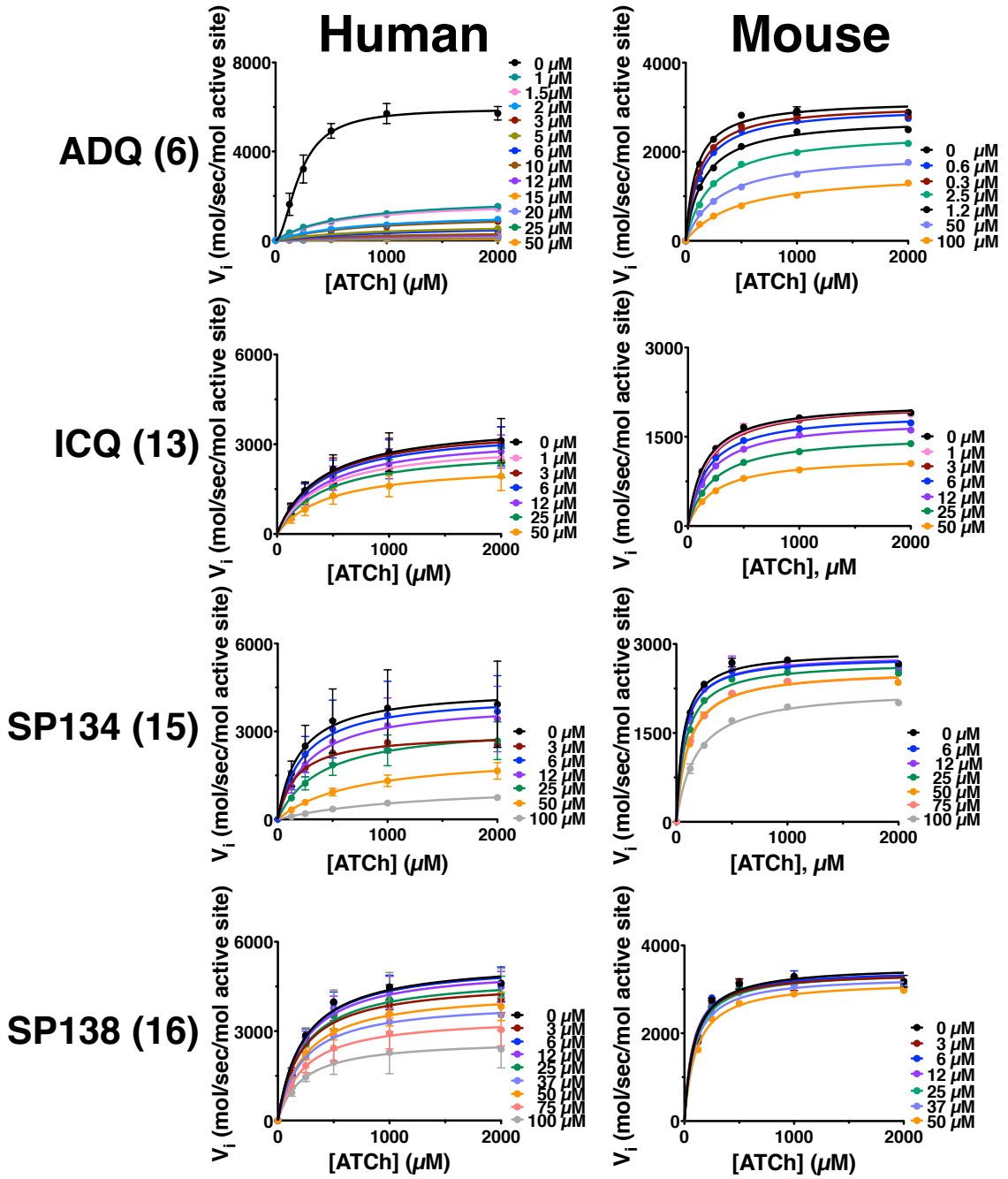

Figure S19. Effect of compounds directly on AChE. In order to determine if the compounds directly effect activity of human (left) or mouse (right) AChE, the compounds were titrated into the enzyme (indicated concentrations at the right of each respective graph) and allowed to come to equilibrium before adding ATCh + DTNB (2mM each, final concentration) and measuring the rate of substrate hydrolysis. Initial rates are plotted at the indicated concentrations of substrate for any given concentration of compound. Any variation of Vmax in the zero compound concentrations was attributed to DMSO that was added to concentration match the DMSO added with a particular compound.

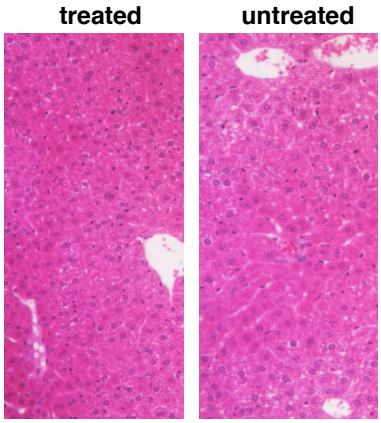

Figure S20. Histology of liver tissue from mice treated (left) or untreated (right) with ADOC (9). Liver tissues from mice given a 120mg/kg dose (same dose that provides protection from lethality) of **ADOC** (**9**) were examined after 2 weeks and showed no signs of necrosis.

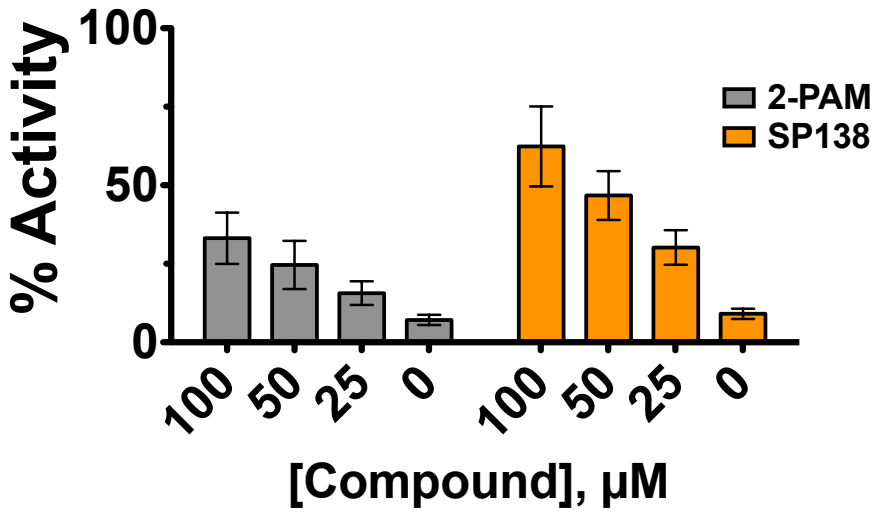

Figure S21. *Ex vivo* tissue reactivation. Animals were treated with a lethal dose of **DFP** (**2**) and their tissues were harvested, homogenized in 1X PBS; 1% TritonX-100 buffer before separating out cell debris. Lysates from the cerebellum were incubated with the indicated concentrations of pralidoxime (**5**), 2-PAM (gray) or **SP138** (**16**) (orange) for 3 hrs at room temperature before adding ATCh and DTNB (2mM each) and determining the amount of activity relative to tissue from animals that had not been challenged with **DFP** (**2**).

Supplementary Tables

Human

	Paraoxon				
	ADQ	**ADOC**	**SP134**	**SP138**	**2-PAM**
k_2(× 10^{-4}), min^{-1}	160 +/- 66	1400+/- 33	70 +/- 0.17	73 +/- 5.2	83 +/- 21
K_R, µM	3.5 +/- 1.6	11 +/- 9.1	11 +/- 6.8	34 +/- 13	75 +/- 16
k_r, $M^{-1}min^{-1}$	4,600+/- 2,900	13,000 +/- 10,000	610 +/- 370	220 +/- 85	110 +/- 37
Hill coeff.	1.0 +/- 0.45	2.8 +/- 0.23	1.8 +/- 0.29	1.3 +/- 0.12	0.88 +/- 0.15
Max. React.	26%	100%	72%	100%	100%

	DFP				
	ADQ	**ADOC**	**SP134**	**SP138**	**2-PAM**
k_2(× 10^{-4}), min^{-1}	21 +/- 1.6	150 +/- 11	32 +/- 1.1	41 +/- 4.0	48 +/- 7.2
K_R, µM	5.8+/-2.0	170+/-100	25 +/- 18	62 +/- 29	430+/-52
k_r, $M^{-1}min^{-1}$	360 +/- 130	89 +/- 55	130 +/- 96	67 +/- 32	11+/- 2.2
Hill coeff.	1.2+/-0.2	1.6+/-0.1	1.8+/- 0.20	1.4 +/- 0.13	1.0+/-0.048
Max. React.	31%	67%	55%	82%	100%

Mouse

	Paraoxon				
	ADQ	**ADOC**	**SP134**	**SP138**	**2-PAM**
k_2(× 10^{-4}), min^{-1}	190 +/- 5.4	7700 +/- 1300	92 +/- 2.8	140 +/- 8.4	3800 +/- 850
K_R, µM	9.1+/- 0.28	110+/- 47	20 +/- 9.8	53 +/- 11	630 +/- 100
k_r, $M^{-1}min^{-1}$	2100+/- 89	7200 +/- 3400	460 +/- 230	270+/- 59	610 +/- 170
Hill coeff.	1.0 +/-0.014	1.7+/-0.11	1.5 +/- 0.13	1.3 +/- 0.065	1.0 +/-0.02
Max. React.	82%	100%	62%	100%	100%

	DFP				
	ADQ	**ADOC**	**SP134**	**SP138**	**2-PAM**
k_2(× 10^{-4}), min^{-1}	---	41+/- 4.4	78 +/- 3.4	82+/- 7.8	100+/- 51
K_R, µM	---	13+/- 9.2	34 +/-35	32 +/- 22	490+/-110
k_r, $M^{-1}min^{-1}$	---	300 +/- 210	220 +/- 230	260 +/- 170	21 +/- 11
Hill coeff.	----	2.0+/-0.3	2.5 +/- 0.31	1.5 +/- 0.22	0.90+/-0.094
Max. React.	----	52%	52%	92%	100%

Table S1. Kinetic parameters calculated from the curves fit to the data shown. Increasing concentrations of reactivation compound were added to OPC inhibited enzyme immediately after separating out excess OPC using a PD10 column. The enzyme was kept cold during chromatography and diluted 1:25 with a phosphate buffer containing BSA to stabilize the enzyme and to dilute out any residual OPC. At various time points after adding reactivator, aliquots were taken and quenched by diluting 1:100. ATCh and DTNB were added immediately to measure activity of the enzyme. The rate of the enzyme (minus any spontaneous reactivation) was set relative to an uninhibited enzyme sample and plotted over time to get the % reactivation over time to get the rate of reactivation. Plots of the dependency of the reactivation compound concentration vs. the rate of reactivation were fit to a one-phase association using the maximum amount of reactivation observed after extended incubation. All reactions were done in duplicate or triplicate and repeated on multiple days and parameters are given +/- standard error. In cases where we have cooperative kinetics, the refinement of values for K_R and by extension k_r is complicated due to the narrow range in concentrations at the inflection point, which contributes to larger errors.

Structure	**apo-AChE**	**DFP-AChE**	**SP134-DFP-AChE**
Space group	$P2_12_12_1$	$P2_12_12_1$	$P2_12_12_1$
Unit cell parameters (*a*, *b*, *c*, α, β, γ)	78.4, 113.1, 227.2, 90, 90, 90	78.6, 114.3, 226.6, 90, 90, 90	79.5, 113.4, 227.1, 90, 90, 90
Resolution (Å)[1]	50-2.0 (2.1-2.0)	50-2.4 (2.5-2.4)	50-2.7 (2.8-2.7)
No. of observations	581,361	320,443	310,251
R_{merge} (%)	7.5 (44.1)	10.9 (45.6)	9.9 (56.9)
Redundancy	4.6 (3.5)	4.0 (3.7)	5.5 (5.6)
I/σI	27.8 (2.5)	21.4 (3.7)	16.2 (2.5)
No. of reflections	126,503	79,533	56,474
Completeness (%)	93 (63)	99 (98)	100 (100)
R_{work} (%)	20.4 (31.6)	21.2 (28.4)	18.3 (27.1)
R_{free}[2] (%)	22.3 (34.5)	23.9 (32.7)	22.1 (31.5)
R.m.s. deviation in bond lengths (Å)	0.008	0.007	0.008
R.m.s. deviation in bond angles (°)	1.3	1.1	1.2

1. The numbers in parentheses are for the highest resolution shell.
2. 5% of the reflections were selected for free *R* calculation.

Table S2. Summary of crystallographic information.

ADOC	
20 min. prior & 5 min. post (60mg/kg ea.)	**5 min. post only (120 mg/kg)**
9/9	6/7

Table S3. Animals treated with ADOC (9). Animals were given **ADOC** (**9**) in two dosing strategies, either 20 minutes prior to challenge with a lethal dose **DFP** (**2**), (3mg/kg) followed by an additional dose 5 minutes afterwards (60mg/kg per dose) or a single dose of 120mg/kg after 5 minutes after challenge. This was done in multiple experiments over a few months time frame. The cumulative results shown are a ratio of those animals that survived 24 hours post-challenge over the total number of animals tested. Cumulatively, 33/35 animals given the same dose of **DFP** (**2**), but without treatment, expired within 100 min.

	Dose	One dose given 1 day prior	Repeated dose for 3 days prior
SP138			
	0.5mg	2/2	---
	1mg	2/2	5/5
	5mg	5/7	3/3
ADQ			
	5mg	3/3	---

Table S4. Animals treated prophylactically. Animals were fed either **ADQ** (**6**) or **SP138** (**16**) mixed in their daily chow prior to challenge with **DFP** (**2**). This was done in multiple experiments over a few months time frame. The results shown are a ratio of those animals that survived 24 hours post-challenge over the total number of animals tested. Cumulatively, 33 out of 35 animals challenged with the same dose of **DFP** (**2**), but without treatment, expired within 100 min. of exposure.

Supporting Information References:

[1] G. L. Ellman, K. D. Courtney, V. Andres, Jr., R. M. Feather-Stone, *Biochemical pharmacology* **1961**, *7*, 88-95.

[2] a)Z. Kovarik, Z. Radic, H. A. Berman, V. Simeon-Rudolf, E. Reiner, P. Taylor, *Biochemistry* **2004**, *43*, 3222-3229; b)A. L. Green, H. J. Smith, *The Biochemical journal* **1958**, *68*, 32-35; c)D. R. Davies, A. L. Green, *The Biochemical journal* **1956**, *63*, 529-535; d)D. M. Maxwell, I. Koplovitz, F. Worek, R. E. Sweeney, *Toxicology and applied pharmacology* **2008**, *231*, 157-164; e)A. Baici, *European journal of biochemistry / FEBS* **1981**, *119*, 9-14; f)C. T. Su, P. H. Wang, R. F. Liu, J. H. Shih, C. Ma, C. H. Lin, C. Y. Liu, M. T. Wu, *Fundamental and applied toxicology : official journal of the Society of Toxicology* **1986**, *6*, 506-514; g)E. I. Wang, P. E. Braid, *The Journal of biological chemistry* **1967**, *242*, 2683-2687; h)F. Worek, P. Eyer, L. Szinicz, *Archives of toxicology* **1998**, *72*, 580-587; i)F. Worek, C. Diepold, P. Eyer, *Archives of toxicology* **1999**, *73*, 7-14.

[3] C. A. Kontogiorgis, D. J. Hadjipavlou-Litina, *Journal of medicinal chemistry* **2005**, *48*, 6400-6408.

[4] P. M. O'Neill, A. Mukhtar, P. A. Stocks, L. E. Randle, S. Hindley, S. A. Ward, R. C. Storr, J. F. Bickley, I. A. O'Neil, J. L. Maggs, R. H. Hughes, P. A. Winstanley, P. G. Bray, B. K. Park, *Journal of medicinal chemistry* **2003**, *46*, 4933-4945.

[5] P. Muthumani, Neckmohammed, Meera, R, Venkataraman, S, Kumar, CA, *Int J Pharm Biomed Res* **2010**, *1*, 78-86.

[6] E.-S. Ibrahim, A. M. Montgomerie, A. H. Sneddon, G. R. Proctor, B. Green, *European Journal of Medicinal Chemistry* **1988**, *23*, 183-188.

[7] G. H. Hakimelahi, K. S. Shia, M. Pasdar, S. Hakimelahi, A. Khalafi-Nezhad, M. N. Soltani, N. W. Mei, H. C. Mei, A. A. Saboury, M. Rezaei-Tavirani, A. A. Moosavi-Movahedi, *Bioorganic & medicinal chemistry* **2002**, *10*, 2927-2932.

[8] Z.-Z. Liu, H.-C. Chen, S.-L. Cao, R.-T. Li, *Synthetic Communications* **1993**, *23*, 2611-2615.

[9] A. Khalafi-Nezhad, M. N. Soltani Rad, G. H. Hakimelahi, B. Mokhtari, *Tetrahedron* **2002**, *58*, 10341-10344.

[10] E. C. Meek, H. W. Chambers, A. Coban, K. E. Funck, R. B. Pringle, M. K. Ross, J. E. Chambers, *Toxicological sciences : an official journal of the Society of Toxicology* **2012**, *126*, 525-533.